

Communication

## Discovery of Fluorogenic Diarylsydnone-Alkene Photo-ligation: Conversion of *ortho*-Dual-Twisted Diarylsydnone into Planar Pyrazolines

linmeng Zhang, Xiaocui Zhang, Zhuojun Yao, Shichao Jiang, Jiajie Deng, Bo Li, and Zhipeng Yu

*J. Am. Chem. Soc.*, **Just Accepted Manuscript** • DOI: 10.1021/jacs.8b02493 • Publication Date (Web): 05 Jun 2018

Downloaded from <http://pubs.acs.org> on June 5, 2018

### Just Accepted

“Just Accepted” manuscripts have been peer-reviewed and accepted for publication. They are posted online prior to technical editing, formatting for publication and author proofing. The American Chemical Society provides “Just Accepted” as a service to the research community to expedite the dissemination of scientific material as soon as possible after acceptance. “Just Accepted” manuscripts appear in full in PDF format accompanied by an HTML abstract. “Just Accepted” manuscripts have been fully peer reviewed, but should not be considered the official version of record. They are citable by the Digital Object Identifier (DOI®). “Just Accepted” is an optional service offered to authors. Therefore, the “Just Accepted” Web site may not include all articles that will be published in the journal. After a manuscript is technically edited and formatted, it will be removed from the “Just Accepted” Web site and published as an ASAP article. Note that technical editing may introduce minor changes to the manuscript text and/or graphics which could affect content, and all legal disclaimers and ethical guidelines that apply to the journal pertain. ACS cannot be held responsible for errors or consequences arising from the use of information contained in these “Just Accepted” manuscripts.

# Discovery of Fluorogenic Diarylsydnone-Alkene Photo-ligation: Conversion of *ortho*-Dual-Twisted Diarylsydnone into Planar Pyrazolines

Linmeng Zhang, Xiaocui Zhang, Zhuojun Yao, Shichao Jiang, Jiajie Deng, Bo Li and Zhipeng Yu\*

Key Laboratory of Green Chemistry and Technology of Ministry of Education, College of Chemistry, Sichuan University, 29 Wangjiang Road, Chengdu 610064, P. R. China

## Supporting Information Placeholder

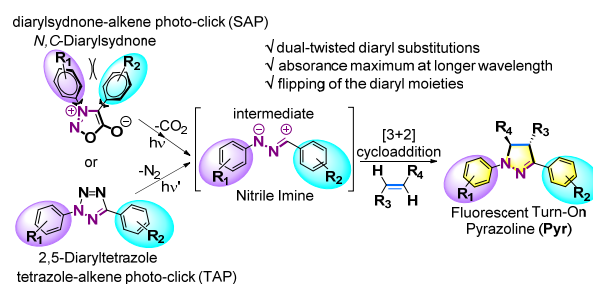
**ABSTRACT:** A small library of diarylsydnone (DASyds) was constructed based on aryl-pairing combinations and subjected to click reaction toward alkenes under photo-irradiation with high efficiency. We were able to demonstrate the utility of DASyds for highly fluorescent turn-on ligation targeting the TCO moieties on protein.

Photo-induced chemoselective covalent-bond forming reactions (photo-click)<sup>1</sup> which introduce probing functionalities are desired tools for materials science<sup>2</sup> to functionalize nanoparticles and interfaces with real-time response, as well as for the labeling of oligonucleotides, proteins, and oligosaccharides.<sup>3</sup> Photon utilization<sup>3a,4</sup> and the precision of the chemistry<sup>4</sup> are both vital for offering better bioorthogonality<sup>5</sup> accompanied with higher spatiotemporal resolution. In spite of this need, only a limited number of photo-click methods have been investigated currently including tetrazole-alkene photo-click chemistry (TAP),<sup>6</sup> photo-initiated thiol-ene,<sup>4c</sup> -yne,<sup>4d</sup> -quinone<sup>4e</sup> reactions, and photo-induced strain-promoted azide-alkyne cycloaddition (photo-SPAAC).<sup>2b</sup> Since the TAP reaction<sup>6</sup> was reported as a bioorthogonal reaction, the photo-click strategy, including [3+2]-type: TAP; photo-SPAAC and the [4+2]-type: *o*-naphthoquinone methides (*o*NQMs)-ene coupling,<sup>4f</sup> has been used to visualize proteins in living cells, to study D(R)NA dynamics,<sup>3c-d</sup> and to track drug molecules.<sup>6c</sup> In spite of the exciting developments over the past two decades, demand remains high for the discovery of new and high-performing photo-click reactions, especially those with the ability to site-specifically hit the desired targets for use in theranostics.

*N*-Phenyl-sydnone were discovered to be clickable with alkynes via copper complex mediation by Taran<sup>7</sup> or strain-promotion by Chin<sup>8a</sup> and Murphy,<sup>8b</sup> and tremendous enhancement of cycloaddition rate achieved via introduction of fluorine substitution by Taran,<sup>8c</sup> elevated this functionality as potential chemical probes to study biomolecular dynamics *in vivo*. Inspired by early sydnone photo-reactions,<sup>9-10</sup> we investigated the photo-induced diarylsydnone-alkene cycloaddition reaction, which affords pyrazoline fluorophores (Scheme 1), as a potentially bioorthogonal conjugation strategy.<sup>5</sup> Since nitrile imine (NI) is the reactive dipolar intermediate,<sup>11</sup> diarylsydnone (DASyds) demonstrate commendable selectivity toward electron-deficient or ring-strained alkenes through a photo-induced transformation sequence.<sup>12</sup> Unlike those in 2,5-diaryltetrazoles, the two *ortho*-substituted aromatic rings in the DASyds scaffold are twisted around the sydnone

core, allowing for unique tuning of reactivity and selectivity of these chemical ligation reagents in 3-D way, as reported herein.

In order to identify a DASyds with excellent photo-response, we consider the electronic effects on the diaryl moieties might be vital to the photo-decarboxylation,<sup>12</sup> including the auxochromes, the polycyclic aromatics (PAR) and the electron donors (eD) or acceptors (eA).<sup>13</sup> Accordingly, a small library of DASyds bearing various aryl substituents on C<sup>4</sup> and N<sup>3</sup> positions were designed (**1a-n**, Figure 1a; **S8-19**, Table S8) and constructed.<sup>14</sup> The UV-Vis spectroscopic properties of representative DASyds were evaluated with maximum absorption wavelengths and the top-three ranked maximum extinction coefficients ( $\epsilon_{\max}$ ) were observed for **1k**>**1j**>**1h** (Figure 1b, Table S1) implying a C<sup>4</sup>-PAR-eA is beneficial. When the N<sup>3</sup>-Ph substituent was an eD, it could offer higher  $\epsilon$  value at  $\lambda_{\max}$  than seen with an eA moiety (**1c** vs. **1d**). This effect on the  $\epsilon$  value was particularly evident when the N<sup>3</sup>-Ph-eD was coupled with a C<sup>4</sup>-Ph-eA, in contrast to a C<sup>4</sup>-Ph-eD (**1e** vs. **1j**) which processes a bathochromic shifting effect. Intriguingly, the absorption peak tail of the simple DASyds could be observed in the visible region (>400 nm, e.g. **1e** and **1f**), which opens the window for visible light-mediated triggering.



**Scheme 1.** The flipping of the diaryl substitutions in the SAP versus TAP.

Subsequent analysis of the photochemistry of the DASyds toward methyl methacrylate in quartz test tube was inquired under exposure to a handheld UV lamp (311 nm, 10.8 mW/cm<sup>2</sup>) or a LED array (371 nm, 15.4 mW/cm<sup>2</sup> or 405 nm, 33.6 mW/cm<sup>2</sup>). Based on HPLC-MS analysis, the experimental results can be summarized as follows: (i) substrates with N<sup>3</sup>-Ph-eA groups (**1b** & **1d**) showed poor reactivity toward alkene (Table 1, entries 2 & 4); (ii) 311 nm irradiation afforded higher conversions for the entire DASyds library (Table 1); (iii) surprisingly, a *p*-aniline moiety on either the N<sup>3</sup> or C<sup>4</sup> positions (e.g., **1e** & **1f**) exhibited very poor photo-response despite their strong absorption at 371 nm and

405 nm (Table 1, entries 5 & 6; Figure S34). Therefore, *N*<sup>3</sup>-*p*-anisole-*C*<sup>4</sup>-Ar-eA-Syds are a better choice for continued screening. Partial hydrolysis of the active intermediate was observed for **1j** and **1k**, accounting for the discrepancy between isolated yield and conversion (Table 1, entries 10 & 11, Figure S11-12) despite their higher conversion at 405 nm. Overall, the three best DASyds at 311 nm irradiation were **1g**, **1h** and **1i** in descending order of reactivity (Table 1, entries 7-9), and no competitive cycloadditions were observed in the dark environment.<sup>15</sup>

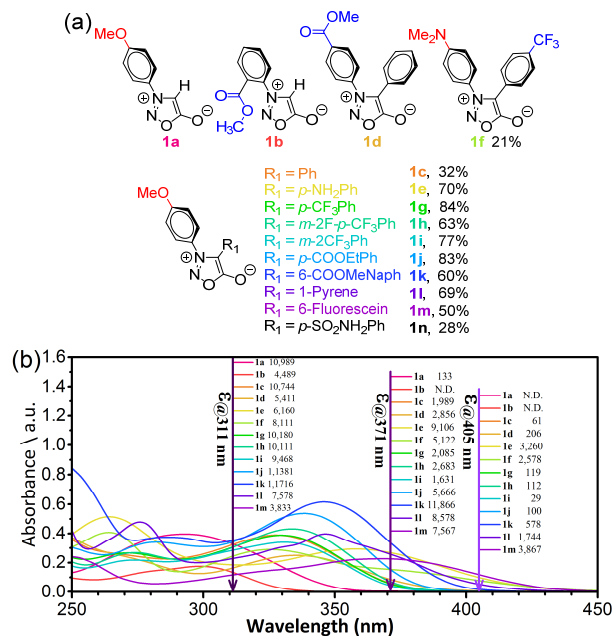


**Figure 1.** (a) Structures of selected DASyds with the C-H activation cross-coupling yield. (b) Absorption spectra and molar absorption coefficients at designated wavelength for selected DASyds from library in acetonitrile/H<sub>2</sub>O (1:1) mixed solvent at 30 μM (250-450 nm).

**Table 1.** Photo-activated 1,3-Dipolar Cycloaddition of **1a-1n** with Methyl Methacrylate<sup>a</sup>

Entry	DASyds		Yield <sup>b</sup> @311 nm	Conv. <sup>c</sup> @311 nm	Conv. <sup>c</sup> @371 nm	Conv. <sup>c</sup> @405 nm
	R <sub>1</sub>	R <sub>2</sub>				
1	<b>1a</b>	<i>p</i> -MeOPh	H	N.D. <sup>d</sup>	97% <sup>e</sup>	-
2	<b>1b</b>	<i>o</i> -COOMePh	H	N.D. <sup>d</sup>	>95% <sup>e</sup>	-
3	<b>1c</b>	<i>p</i> -MeOPh	Ph	55%	92% <sup>d</sup>	47% <sup>d</sup>
4	<b>1d</b>	<i>p</i> -COOMePh	Ph	Trace	90% <sup>d</sup>	80% <sup>d</sup>
5	<b>1e</b>	<i>p</i> -MeOPh	<i>p</i> -NH <sub>2</sub> Ph	Trace	14%	11%
6	<b>1f</b>	<i>p</i> -Me <sub>2</sub> NPh	<i>p</i> -CF <sub>3</sub> Ph	Trace	17%	N.D. <sup>d</sup>
7	<b>1g</b>	<i>p</i> -MeOPh	<i>p</i> -CF <sub>3</sub> Ph	83% <sup>e</sup>	95%	43%
8	<b>1h</b>	<i>p</i> -MeOPh	<i>m</i> -2F- <i>p</i> -CF <sub>3</sub> Ph	71%	94%	48%
9	<b>1i</b>	<i>p</i> -MeOPh	<i>m</i> -2CF <sub>3</sub> Ph	70%	92%	47%
10	<b>1j</b>	<i>p</i> -MeOPh	<i>p</i> -COOEtPh	75%	95% <sup>h</sup>	61% <sup>h</sup>
11	<b>1k</b>	<i>p</i> -MeOPh	6-COOMeNaph	70%	92% <sup>h</sup>	77% <sup>h</sup>
12	<b>1m</b>	<i>p</i> -MeOPh	6-Fluorescein	-	95% <sup>h</sup>	79% <sup>h</sup>
13	<b>1n</b>	<i>p</i> -MeOPh	<i>p</i> -SO <sub>2</sub> NH <sub>2</sub> Ph	69% <sup>e</sup>	90%	51%

<sup>a</sup>5 mg of **1** and 20 eq. of MMA in 10 mL of ethyl acetate (EtOAc) with 311 nm UV for 2 h unless noted otherwise. <sup>b</sup>Isolated yield. <sup>c</sup>100 μM **1** and 2 mM **2a** in ACN/H<sub>2</sub>O (1:1) was irradiated with designated light source for 60s. Determined by LC-MS. See Figure S2-14 for details. <sup>d</sup>N.D. = not detected. <sup>e</sup>All converted into undesired products. <sup>f</sup>By-products formed. <sup>g</sup>30 mg of **1** in 50 mL of EtOAc scale. <sup>h</sup>Hydrolysis as a predominate side-reaction.

Only a single regioisomer of **3ga** was observed based on the <sup>1</sup>H NMR signals of the Pyr protons and XRD structure, thus verifying the synergistic occurrence of geometric flipping and planarization with the photo-reaction (Table 1; Figure S34). Compared to the DASyds (**1g**, **1i**, **1j**), the corresponding 2,5-diaryltetrazole has an hypsochromic shift of absorbance peak around 37-48 nm, resulting in its complete inertness under excitation by 371 nm LED (Figure S23).

To expand the scope of reporters<sup>16</sup> paired with **1g**, we examined the photo-induced ligation by incubating **1g** with a range of representative alkenes upon 311 nm irradiation (10.8 mW/cm<sup>2</sup>) (Table 2). As expected, electron-deficient alkenes, such as **2a** and **2d** (diethyl fumarate, DEF), reacted efficiently with **1g** within 2h, furnishing high yields, despite concomitant formation of the corresponding pyrazole as an oxidative aromatization product, especially for DEF (Table 2, entry 4, page 153 in SI). Alternatively, alkene **2c** (norbornene, NOR) exhibited a relative low yield (66%, Table 2, entry 3, Figure S16) mainly because of side-reactions. The genetic encodable ring-strained *trans*-cyclooct-4-en-1-ol (TCO)<sup>4a</sup> appears to be promising, undergoing the photo-click reaction to form **3gb** (Table 2, entry 2), superior not only in ligation precision but also satisfying Φ<sub>F</sub> (up to 42%). Unexpectedly, **2e** (5-vinyl-2'-deoxyuridine, VdU)<sup>17</sup> behaves as a good ligation substrate with respect to **1g**, affording a 68% yield of **3ge** with little oxidation. The slightly lower yield is caused by incomplete conversion of **1g** because of the extra optical filtering effect from VdU (Table 2, entry 5).<sup>18</sup> Significant bathochromic shift of absorption (λ<sub>max</sub> shifted from 33 to 66 nm), arising in emission maxima (λ<sub>em</sub>, from 525 to 543 nm), accompanied with large Stokes' shifts (Δλ, from 158 to 163 nm) were spectroscopic characteristics of fluorophores, **3ga-3ge**, upon isolation (Table 2).

**Table 2.** Photo-activated 1,3-Dipolar Cycloaddition of **1g** with Various Alkene Dipolarophiles<sup>a</sup>

Entry	Alkene	λ <sub>max</sub> /λ <sub>em</sub> (nm)	Φ <sub>F</sub> /ε <sub>max</sub> <sup>b</sup>	Stoke shift	Yield <sup>d</sup> (%)	Conv. <sup>f</sup> (%)
1	<b>2a</b>	367/525	0.56/15.9	158 nm	83	94
2	<b>2b</b>	376/534	0.42/11.2	158 nm	85	97
3	<b>2c</b>	396/533	0.35/18.9	137 nm	66	91 <sup>g</sup>
4	<b>2d</b>	380/543	0.22/17.1	163 nm	78 <sup>d</sup> (9 <sup>e</sup> )	95
5	<b>2e</b>	381/534	0.16/15.2	153 nm	68	46 <sup>g</sup>

<sup>a</sup>Irradiation 20 mg of **1g** and 5 eq. of alkenes in 50 mL of EtOAc for 2h. <sup>b</sup>Φ<sub>F</sub> denote fluorescence quantum yield, ε<sub>max</sub> in 10<sup>3</sup> M<sup>-1</sup>cm<sup>-1</sup>. <sup>c</sup>Isolated yields. <sup>d</sup>20 eq. DEF. <sup>e</sup>Side-product from oxidative aromatization. <sup>f</sup>100 μM **1g** and 0.5 mM **2** in ACN/H<sub>2</sub>O (1:1), 311 nm UV for 60s. Determined by LC-MS. See Figure S15-18 for details. <sup>g</sup>Not peak-to-peak conversion.

Encouraged by the high efficiency of the photo-reaction, we continued to determine the magnitude of fluorescence turn-on effect derived from preferred DASyds, **1g-1i**, toward TCO under irradiation at 371 nm (15.4 mW/cm<sup>2</sup>), appending corresponding photophysical properties of the resultant Pyrs (Table 3). Likewise, the chromophoric and fluorophoric nature of products **3gb-3ib** in the visible range allowed for facile visualization of their formation. Three DASyds show excellent degrees of fluorescence turn-on effect, ranging from 122-fold for **3gb** to 321-fold for **3ib** (Table 3).<sup>15</sup> As displayed in Figure 2, complete photo-conversion to the desired Pyr **3hb** was achieved within 520s as evidenced by the

iterative increase in a new absorption peak at 397 nm and a broad emission peak centered at 553 nm simultaneously. Complete conversion to **3gb** requires longer time than **3hb**, but still proceeds within a similar scale (for turn-on ratio in ACN:PBS = 1:2, pH~7.4, also see Figure S19-S21). Overall, DASyds **1g-1i** hold great potential for fluorogenic imaging.

The plausible mechanism of the DASyds-alkene photo-reaction was proposed,<sup>12</sup> but the reaction rate as a ligation method has not been investigated. We probed the rate profile by capturing time-dependent fluorescence evolution under LED irradiation (371 nm, 28.0 mW/cm<sup>2</sup>, Figure S1) via monitoring the  $\lambda_{em}$  signal of corresponding Pyr product. Unexpectedly, the apparent first-order rate constant,  $k_{obs}$ , detected for **1g-1i** with either TCO or NOR were almost equal ( $k_{obs1g-TCO} = 0.045 \text{ s}^{-1}$  vs.  $k_{obs1g-NOR} = 0.044 \text{ s}^{-1}$ , Figure S1), independent on the alkene type or concentration but dependent on the DASyds itself ( $k_{obs1g-TCO} = 0.045 \text{ s}^{-1}$  vs.  $k_{obs1i-TCO} = 0.034 \text{ s}^{-1}$ , Table 3), implying that the decarboxylation of 4,5-dioryl-2-oxa-1,5-diazabicyclo[2.1.0]pentan-3-one<sup>12b</sup> (Figure S1) might become the rate determining step instead of the ultra-fast [3+2] cycloaddition<sup>11</sup> (Figure S1). The quantum yields of the photo-chemical reaction for **1g**, **1h**, and **1i** were determined to be 0.20, 0.10, and 0.12, respectively (for yield in ACN:PBS = 1:2, pH~7.4, also see Figure S25).

**Table 3.** Photophysical Properties of the TCO-Pyrs and Fluorescence Turn-On Efficiency<sup>a</sup>

Comp.	$\lambda_{max}/\lambda_{em}$ <sup>b</sup> (nm)	$\epsilon_{max}$ <sup>c</sup>	$\epsilon_{400nm}$ <sup>c</sup>	$\Phi_F$ <sup>d</sup>	$\Phi_R$ <sup>e</sup>	$k_{obs}$ <sup>f</sup> (s <sup>-1</sup> )	Fluorescence turn-on <sup>g</sup>
<b>1g</b>	331/-	13,573	347	N.D.	0.20	0.045	122-fold
<b>3gb</b>	376/532	11,156	8,100	0.42			
<b>1h</b>	334/-	15,333	213	N.D.	0.10	0.043	205-fold
<b>3hb</b>	396/552	18,533	18,400	0.33			
<b>1i</b>	331/-	11,853	187	N.D.	0.12	0.034	321-fold
<b>3ib</b>	383/543	13,178	11,611	0.28			

<sup>a</sup>25  $\mu\text{M}$  **1g-1i** in ACN/H<sub>2</sub>O (1:1). <sup>b</sup> $\lambda_{max}$  in the 300-500 nm region. <sup>c</sup> $\text{M}^{-1}\text{cm}^{-1}$ . <sup>d</sup>Fluorescence quantum yield in EtOAc. <sup>e</sup>Reaction quantum yield. <sup>f</sup>Obtained by comparing the emission intensity of Pyr to that of the initial reactants mixture at  $\lambda_{em}$ ;  $\lambda_{ex} = 400 \text{ nm}$ .

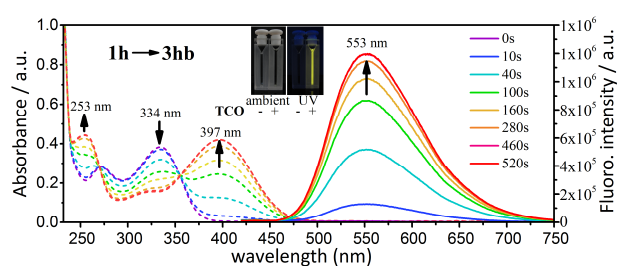


**Figure 2.** Time course of photo-ligation of TCO-DASyds as monitored by UV-vis (dashed lines) and fluorescence (solid lines). **1h** in ACN/H<sub>2</sub>O (1:1) to derive concentrations of 25  $\mu\text{M}$ , and the activation wavelength was set at 365 nm (0.95 mW/cm<sup>2</sup>). For fluorescence,  $\lambda_{ex} = 400 \text{ nm}$ .

To demonstrate the utility of the DASyds for bioconjugation, we first appended the TCO moiety to lysozyme (lyso-TCO, M.W. ~14.3 kDa) via chemical tagging and to sfGFP via genetic incorporation (sfGFP-Q204TCOK, M.W. ~27.9 kDa).<sup>19</sup> Then, the residue-specific protein modification was investigated by reacting the resultant proteins with **1g** and **1k** under irradiation of 311 nm and 405 nm light for 2 min, respectively. The resultant mixture was profiled by in-gel fluorescence imaging (Figure 3a-b) and LC-MS (Figure 3c). The conversions into lyso-Pyr-**1g** or lyso-Pyr-**1k** or

sfGFP-Pyr-**1g** were estimated to be 40%, 32% and 14% (Figure S26-32, S35-36) with 1.8%, 4.4% and 8.1% of non-specific reactions respectively. The LC-MS/MS analysis revealed that the photo-ligation reaction of **1g** has a highly spatial preference toward K97-TCO residue of lyso-TCO (Figure S33). In-gel fluorescence imaging indicated obvious fluorescent turn-on bands only for lanes meeting all requirements for the photo-ligation (Figure 3a-b).

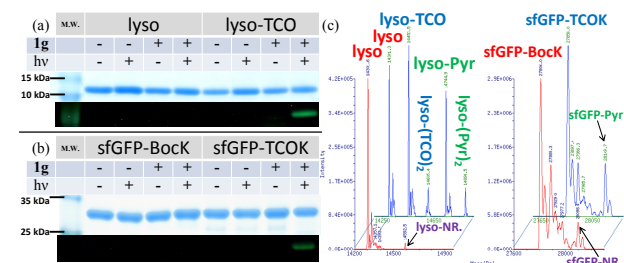


**Figure 3.** Selective photo-induced fluorogenic labeling of proteins by **1g** *in vitro*. Coomassie blue stain (top panel) and in-gel fluorescence (bottom panel) of the same protein gel after resolved by SDS-PAGE (a) lyso (b) sfGFP. (c) Deconvoluted mass spectra of control protein (red) and the TCO-protein mixture (blue) showing the formation of the Pyr adduct (green). NR = non-specific reaction (purple).

In summary, with a small library of photo-activatable DASyds in hand, we were able to identify **1g-1i** as excellent candidates for photo-clickable fluorogenic ligation. The **1g** showed high reactivity toward TCO and TCO-containing proteins when exposed to near-UV light, giving rise to fluorescent Pyr cycloadducts with outstanding ratio of fluorescence turn-on effect. We will consider the applications of DASyds derivatives as light-activable reagents for ligation reaction in living systems.

## ASSOCIATED CONTENT

### Supporting Information

The Supporting Information is available free of charge on the ACS Publications website at DOI:

Experimental details, characterization of all new compounds, and computational results (PDF).

X-ray crystal structure of **1f** (CCDC-1556441) (CIF)

X-ray crystal structure of **1g** (CCDC-1556442) (CIF)

X-ray crystal structure of **1m** (CCDC-1823237) (CIF)

X-ray crystal structure of **3ga** (CCDC-1556443) (CIF)

## AUTHOR INFORMATION

### Corresponding Author

zhipengy@scu.edu.cn

### ORCID

Zhipeng Yu: 0000-0001-6411-6078

### Notes

The authors declare no competing financial interests.

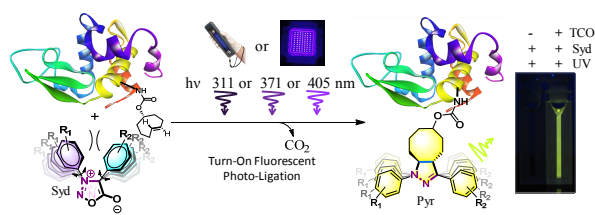
## ACKNOWLEDGMENT

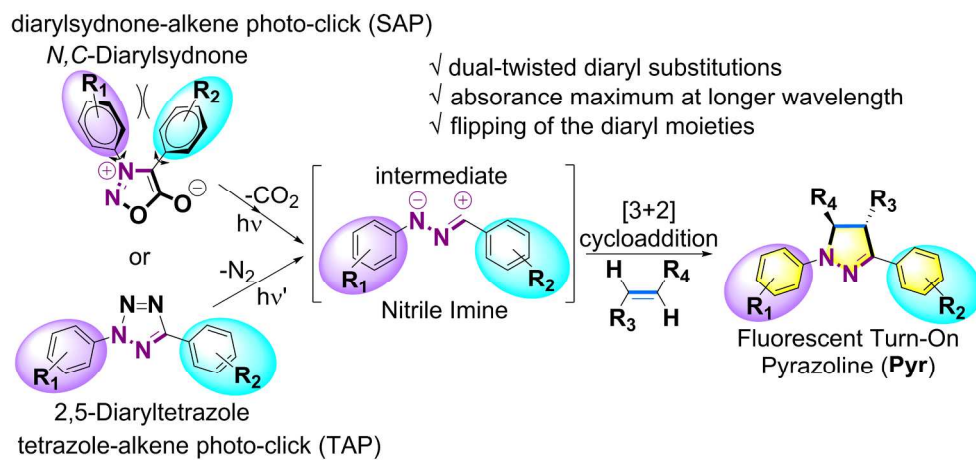
We thank Dr. Jason J. Chruma (Sichuan University) for valuable help and suggestions in manuscript preparation. We thank Dr. Wenshe Liu (Texas A&M) and Dr. Qing Lin (SUNY-UB) for generously providing us the plasmids pEvol-PyIT-PyIRS and pET-sfGFP-Q204TAG. We thank Dr. Pengchi Deng (Analytical & Testing Center, SCU) for help on NMR spectra collection. Financial support was provided by the National Natural Science Foundation of China (21502130), the "1000-Youth Talents Pro-

gram”, and the Fundamental Research Funds for the Central Universities.

## REFERENCES

- (1) Tasdelen, M. A.; Yagci, Y. *Angew. Chem. Int. Ed.* **2013**, *52*, 5930–5938.
- (2) (a) Voskuhl, J.; Brinkmann, J.; Jonkheijm, P. *Curr. Opin. Chem. Biol.* **2014**, *18*, 1–7. (b) McNitt, C. D.; Cheng, H.; Ullrich, S.; Popik, V. V.; Bjerknes, M. *J. Am. Chem. Soc.* **2017**, *139*, 14029–14032. (c) He, M.; Li, J.; Tan, S.; Wang, R.; Zhang, Y. *J. Am. Chem. Soc.* **2013**, *135*, 18718–18721. (d) Yagci, Y.; Jockusch, S.; Turro, N. J. *Macromolecules* **2010**, *43*, 6245–6260.
- (3) (a) Herner, A.; Lin, Q. *Top. Curr. Chem.* **2016**, *374*, 1–31. (b) Whitehead, S. A.; McNitt, C. D.; Mattern-Schain, S. I.; Carr, A. J.; Alam, S.; Popik, V. V.; Best, M. D. *Bioconjugate Chem.* **2017**, *28*, 923–932. (c) Nainar, S.; Kubota, M.; McNitt, C.; Tran, C.; Popik, V. V.; Spitale, R. C. *J. Am. Chem. Soc.* **2017**, *139*, 8090–8093. (d) Li, J.; Huang, L.; Xiao, X.; Chen, Y.; Wang, X.; Zhou, Z.; Zhang, C.; Zhang, Y. *J. Am. Chem. Soc.* **2016**, *138*, 15943–15949.
- (4) (a) Zhang, H.; Trout, W. S.; Liu, S.; Andrade, G. A.; Hudson, D. A.; Scinto, S. L.; Dicker, K. T.; Li, Y.; Lazouski, N.; Rosenthal, J.; Thorpe, C.; Jia, X.; Fox, J. M. *J. Am. Chem. Soc.* **2016**, *138*, 5978–5983. (b) Yu, Z.; Ohulchanskyy, T. Y.; An, P.; Prasad, P. N.; Lin, Q. *J. Am. Chem. Soc.* **2013**, *135*, 16766–16769. (c) Killops, K. L.; Campos, L. M.; Hawker, C. J. *J. Am. Chem. Soc.* **2008**, *130*, 5062–5064. (d) Hensarling, R. M.; Doughty, V. A.; Chan, J. W.; Patton, D. L. *J. Am. Chem. Soc.* **2009**, *131*, 14673–14675. (e) Arumugam, S.; Popik, V. V. *J. Am. Chem. Soc.* **2012**, *134*, 8408–8411. (f) Arumugam, S.; Orski, S. V.; Locklin, J.; Popik, V. V. *J. Am. Chem. Soc.* **2012**, *134*, 179–182. (g) Adzima, B. J.; Tao, Y.; Kloxin, C. J.; DeForest, C. A.; Anseth, K. S.; Bowman, C. N. *Nat. Chem.* **2011**, *3*, 256–259.
- (5) J. A. Prescher, C. R. Bertozzi, *Nat. Chem. Biol.* **2005**, *1*, 13–21.
- (6) (a) Wang, Y.; Song, W.; Hu, W. J.; Lin, Q. *Angew. Chem. Int. Ed.* **2009**, *48*, 5330–5333. (b) Yu, Z.; Lin, Q. *J. Am. Chem. Soc.* **2014**, *136*, 4153–4156. (c) Yu, Z.; Ho, L. Y.; Lin, Q. *J. Am. Chem. Soc.* **2011**, *133*, 11912–11915.
- (7) Kolodych, S.; Rasolofonjatovo, E.; Chaumontet, M.; Nevers, M.-C.; Créminon, C.; F. Taran, *Angew. Chem. Int. Ed.* **2013**, *52*, 12056–12060.
- (8) (a) Wallace, S.; Chin, J. W. *Chem. Sci.* **2014**, *5*, 1742–1744. (b) Narayanam, M. K.; Liang, Y.; Houk, K. N.; Murphy, J. M. *Chem. Sci.* **2016**, *7*, 1257–1261. (c) Liu, H.; Audisio, D.; Plougastel, L.; Decuypere, E.; Buisson, D.-A.; Koniev, O.; Kolodych, S.; Wagner, A.; Elhabiri, M.; Krzyczmonik, A.; Forsback, S.; Solin, O.; Gouverneur, V.; Taran, F. *Angew. Chem. Int. Ed.* **2016**, *55*, 12073–12077.
- (9) (a) Huseya, Y.; Chinone, A.; Ohta, M. *Bull. Chem. Soc. Jpn.* **1971**, *44*, 1667–1668. (b) Märky, M.; Hansen, H.-J.; Schmid, H. *Helv. Chim. Acta* **1971**, *54*, 1275–1278. (c) Pfoertner, K.-H.; Foricher, J. *Helv. Chim. Acta* **1980**, *63*, 653–657. (d) George, M. V.; Angadiyavar, C. S. *J. Org. Chem.* **1971**, *36*, 1589–1594. (e) Gotthardt, H.; Reiter, F. *Tetrahedron Lett.* **1971**, *12*, 2749–2752.
- (10) Butković, K.; Vuk, D.; Marinić, Ž.; Penić, J.; Šindler-Kulyk, M. *Tetrahedron* **2010**, *66*, 9356–9362.
- (11) (a) Wang, X. S.; Lee, Y.; Liu, W. R. *Chem. Commun.* **2014**, *50*, 3176–3179. (b) Kauffmann, T.; Berger, D.; Scheerer, B.; Woltermann, A. *Chem. Ber.* **1977**, *110*, 3034–3039.
- (12) (a) Krauch, C. H.; Kuhls, J.; Piek, H.-J. *Tetrahedron Lett.* **1966**, *7*, 4043–4048. (b) Veedu, R. N.; Kvaskoff, D.; Wentrup, C. *Aust. J. Chem.* **2014**, *67*, 457–468.
- (13) Bixon, M.; Jortner, M. *Adv. Chem. Phys.* **1999**, *106*, 35–202.
- (14) (a) Browne, D. L.; Vivat, J. F.; Plant, A.; Gomez-Bengoa, E.; Harrity, J. P. A. *J. Am. Chem. Soc.* **2009**, *131*, 7762–7769. (b) Delaunay, T.; Genix, P.; Es-Sayed, M.; Vors, J.-P.; Monteiro, N.; Balme, G. *Org. Lett.* **2010**, *12*, 3328–3331. (c) Brown, A. W.; Harrity, J. P. A. *J. Org. Chem.* **2015**, *80*, 2467–2472. (d) Specklin, S.; Decuypere, E.; Plougastel, L.; Aliani, S.; Taran, F. *J. Org. Chem.* **2014**, *79*, 7772–7777.
- (15) The competitive thermal cycloaddition reactions with TCO and MMA in dark are extremely slow at 25 °C (Figure S22).
- (16) (a) Grammel, M.; Hang, H. C. *Nat. Chem. Biol.* **2013**, *9*, 475–484. (b) Patterson, D. M.; Nazarova, L. A.; Xie, B.; Kamber, D. N.; Prescher, J. A. *J. Am. Chem. Soc.* **2012**, *134*, 18638–18643.
- (17) (a) Rieder, U.; Luedtke, N. W. *Angew. Chem., Int. Ed.* **2014**, *53*, 9168–9172. (b) Nguyen, K.; Fazio, M.; Kubota, M.; Nainar, S.; Feng, C.; Li, X.; Atwood, S. X.; Bredy, T. W.; Spitale, R. C. *J. Am. Chem. Soc.* **2017**, *139*, 2148–2151. VdU is a surrogate for thymidine both *in vitro* and *in vivo*.
- (18) MacDonald, B. C.; Lvin, S. J.; Patterson, H. *Analytica Chimica Acta.* **1997**, *338*, 155–162.
- (19) Lee, Y. J.; Wu, B.; Raymond, J. E.; Zeng, Y.; Fang, X.; Wooley, K. L.; Liu, W. R. *ACS Chem. Biol.* **2013**, *8*, 1664–1670.





**Scheme 1.** The flipping of the diaryl substitutions in the SAP versus TAP.

411x186mm (144 x 144 DPI)

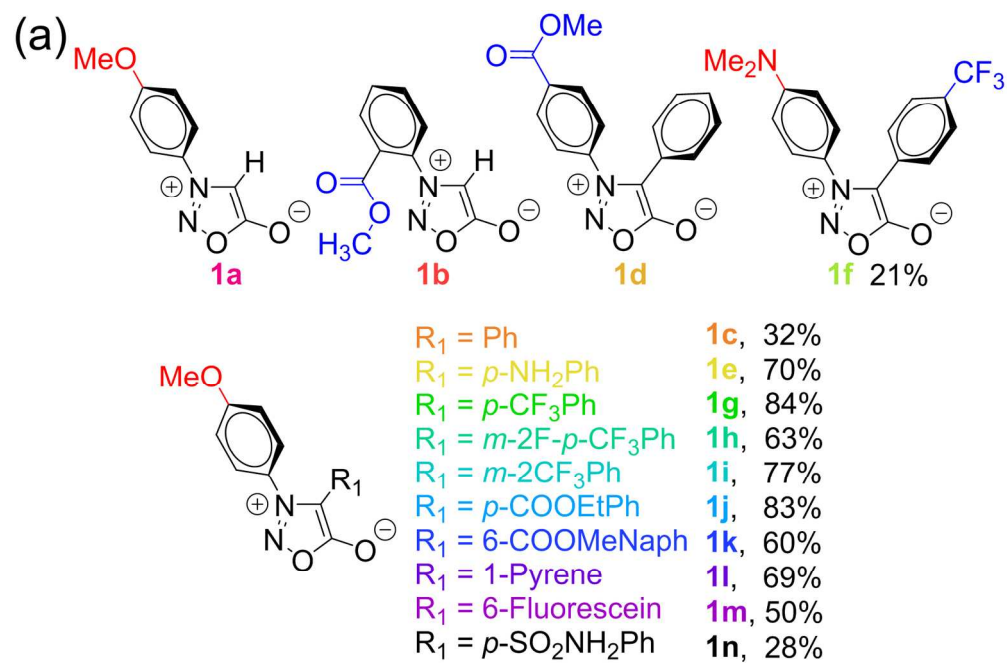
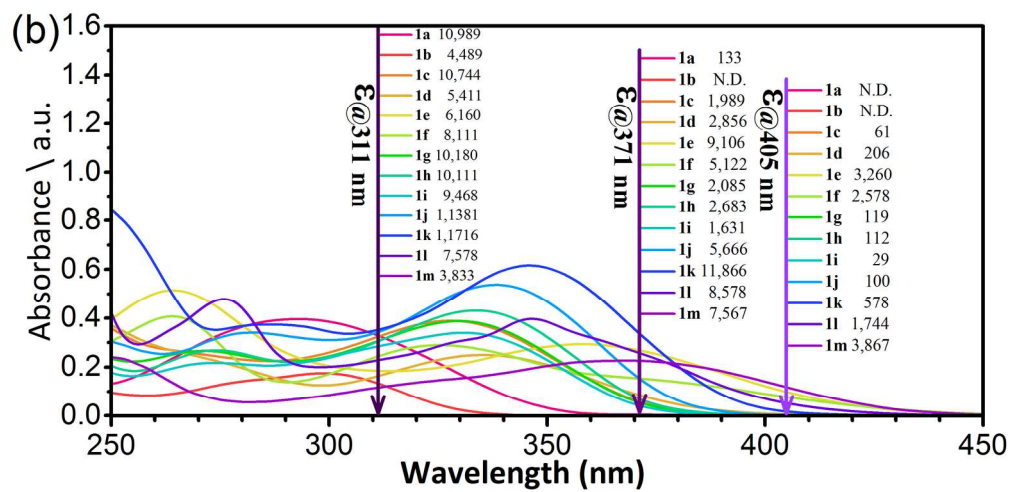


**Figure 1.** (a) Structures of selected DASyds with the C-H activation cross-coupling yield.

339x221mm (144 x 144 DPI)



23 **Figure 1.** (b) Absorption spectra and molar absorption coefficients at designated wavelength for selected  
24 DASyds from library in acetonitrile/H<sub>2</sub>O (1:1) mixed solvent at 30  $\mu$ M (250-450 nm).

25 409x197mm (144 x 144 DPI)

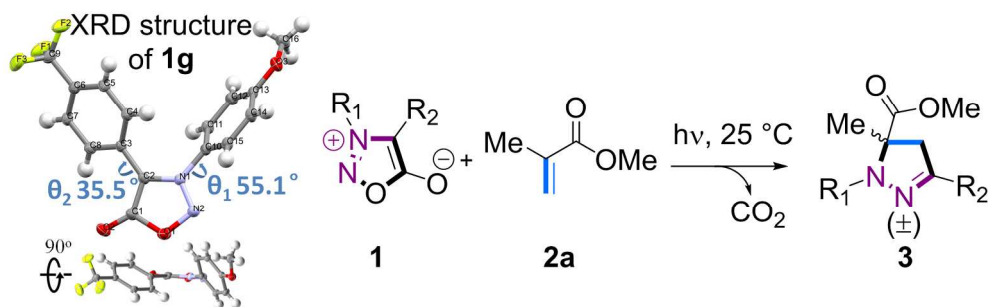


**Table 1.** Photo-activated 1,3-Dipolar Cycloaddition of **1a-1n** with Methyl Methacrylate

398x123mm (144 x 144 DPI)

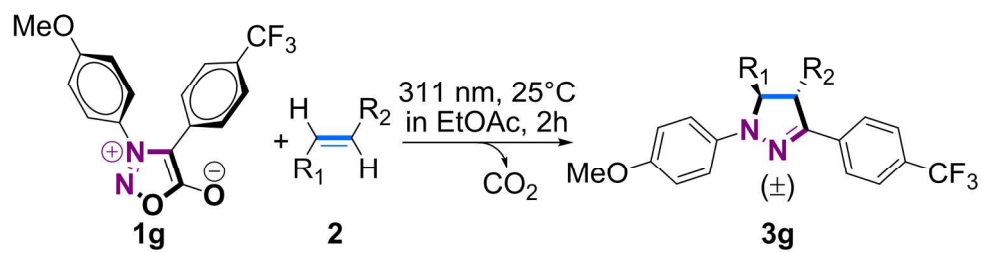
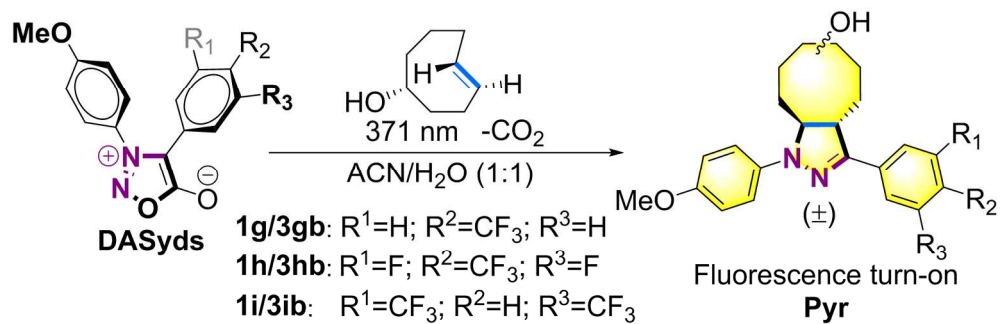


**Table 2.** Photo-activated 1,3-Dipolar Cycloaddition of **1g** with Various Alkene Dipolarophiles

379x95mm (144 x 144 DPI)



18 **Table 3.** Photophysical Properties of the TCO-Pyrs and Fluorescence Turn-On Efficiency

19  
20 360x117mm (144 x 144 DPI)

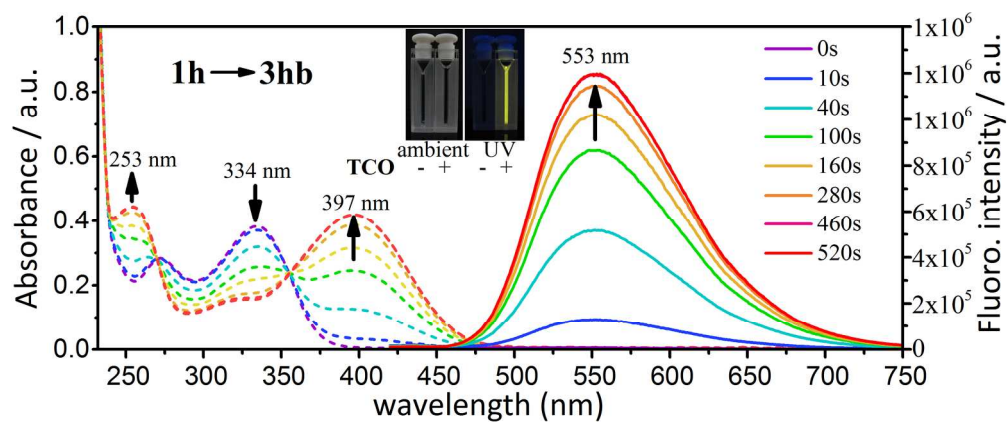


**Figure 2.** Time course of photo-ligation of TCO-DASyd as monitored by UV-vis (dashed lines) and fluorescence (solid lines). DASyd in ACN/H<sub>2</sub>O (1:1) to derive concentrations of 25  $\mu$ M, and the activation wavelength was set at 365 nm (0.95 mW/cm<sup>2</sup>). For fluorescence,  $\lambda_{\text{ex}}$  = 400 nm.

414x171mm (144 x 144 DPI)

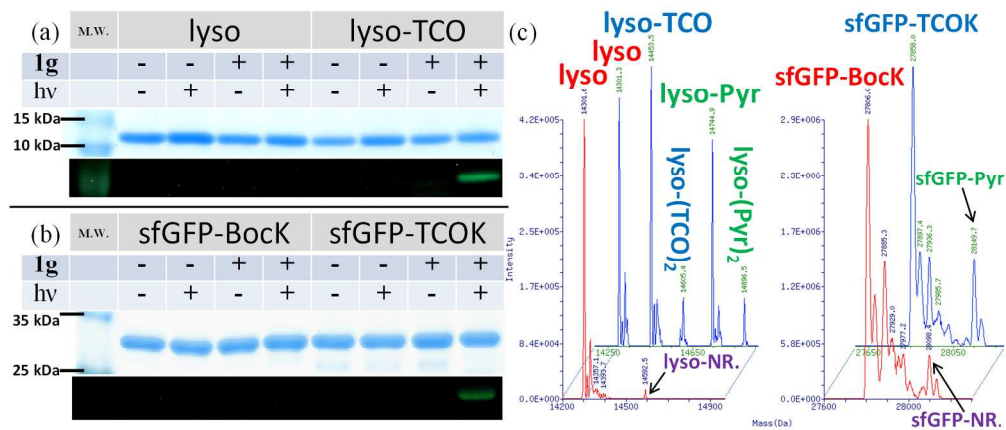


**Figure 3.** Selective photo-induced fluorogenic labeling of proteins by **1g** *in vitro*. Coomassie blue stain (top panel) and in-gel fluorescence (bottom panel) of the same protein gel after resolved by SDS-PAGE (a) lyso (b) sfGFP. (c) Deconvoluted mass spectra of control protein (red) and the TCO-protein mixture (blue) showing the formation of the Pyr adduct (green). NR. = non-specific reaction (purple).

413x178mm (144 x 144 DPI)

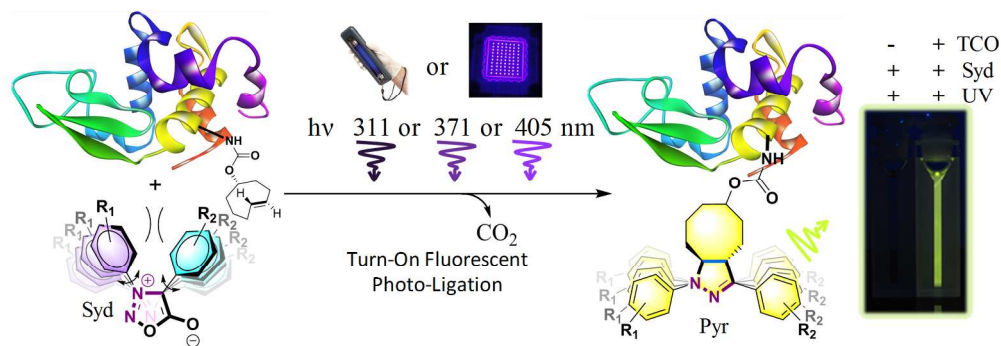


Table of Contents

403x137mm (144 x 144 DPI)

1  
2  
3  
4  
5  
6  
7  
8  
9  
10  
11  
12  
13  
14  
15  
16  
17  
18  
19  
20  
21  
22  
23  
24  
25  
26  
27  
28  
29  
30  
31  
32  
33  
34  
35  
36  
37  
38  
39  
40  
41  
42  
43  
44  
45  
46  
47  
48  
49  
50  
51  
52  
53  
54  
55  
56  
57  
58  
59  
60